

Scanning tunneling spectroscopy characterization of the pseudogap and the $x = \frac{1}{8}$ anomaly in $La_{2-x}Sr_xCuO_4$ thin films

Ofer Yuli, Itay Asulin, and Oded Millo*

Racah Institute of Physics, The Hebrew University of Jerusalem, Jerusalem 91904, Israel

Gad Koren

Department of Physics, Technion - Israel Institute of Technology, Haifa 32000, Israel

Abstract

Using scanning tunneling spectroscopy we examined the local density of states of thin c -axis $La_{2-x}Sr_xCuO_4$ films, over wide doping and temperature ranges. We found that the pseudogap exists only at doping levels lower than optimal. For $x = 0.12$, close to the 'anomalous' $x = \frac{1}{8}$ doping level, a zero bias conductance peak was the dominant spectral feature, instead of the expected V-shaped (c -axis tunneling) gap structure. We have established that this surprising effect cannot be explained by tunneling into (110) facets. Possible origins for this unique behavior are discussed.

PACS numbers: 74.72.Dn, 74.50.+r, 74.78.Bz, 74.25.Jb

*Electronic address: milode@vms.huji.ac.il

I. INTRODUCTION

For a certain doping range, at temperatures higher than the superconducting transition temperature T_c , hole doped cuprate high temperature superconductors (HTSC) exhibit depletion in the density of states (DOS) around the Fermi energy, E_F . This 'soft gap', known as the pseudogap (PG) persists up to a doping dependent temperature $T^* > T_c$. The PG phenomenon is not yet well understood and it is even still unclear whether its origin is related to superconductivity or not. Experimentally, the PG has been studied extensively for different HTSCs, using various methods. [1] Several experiments show that the PG exists only in the underdoped regime and that there, for each doping level, it evolves smoothly into the superconducting (SC) gap at the corresponding T_c . This suggests that both phases share a similar energy scale. In contrast, quite a few studies reveal deviations from the above 'universal' behavior. Angle resolved photo emission spectroscopy (ARPES) investigations [2, 3] imply that there may be two PGs of different origins in $La_{2-x}Sr_xCuO_4$ (LSCO), with typical gap values of ~ 30 and ~ 100 meV. Scanning tunneling microscopy and spectroscopy (STM and STS) studies of Bi-based cuprates show that the PG extends into the overdoped regime, [4, 5] while no PG has been measured for optimally- and overdoped $YBa_2Cu_3O_{7-\delta}$ (YBCO). [6] These contradicting data raise the question of whether the observed results are truly universal attributes of the PG in the HTSC cuprates.

STS enables precise measurements of the single particle excitation spectra, with high energy and spatial resolution, making it a powerful tool for studying the energy scales of both the SC gap and the PG. Atomically-resolved STS measurements of the DOS in $Bi_2Sr_2CaCu_2O_{8-\delta}$ (BSCCO) revealed large spatial fluctuations of the quasi-particle DOS [7, 8, 9, 10] and provided the first tunneling spectroscopy data of the PG doping and temperature dependencies. [4] In fact, most of the STS investigations of the cuprates has been performed on BSCCO due to the relative ease of achieving a clean surface by cleavage under vacuum. In contrast, very few STM studies have been carried out on LSCO due to problems of surface degradation. The same problem also hindered STM measurements of heavily underdoped YBCO.

The relatively low T_c and ease of sample preparation over a wide doping range make LSCO an ideal candidate for studying the PG. This is illustrated by the abundant experimental data available, acquired using various techniques such as transport measurements,

[11] point contact spectroscopy [12], tunnel junctions, [13] infra red spectroscopy, [14] and ARPES. [15] It is therefore unfortunate that STS measurements on LSCO are relatively scarce, and were performed mainly on optimally doped samples. Obviously, it is very important to expand the STS measurements in LSCO also to the under- and overdoped regimes of the phase diagram, to obtain a comprehensive picture of the doping dependence of the DOS and elucidate the relation between the SC and PG states. This will hopefully be an important step towards resolving the mechanism underlying high T_c superconductivity.

Another unresolved property of LSCO and related cuprates (e.g. the La-214 family) is the $x = \frac{1}{8}$ anomaly, where a suppression of the superconducting transition temperature is observed. This is manifested in $La_{2-x}Ba_xCuO_4$ [16] where T_c drops to nearly zero at $x = \frac{1}{8}$, and in LSCO, in a more subtle way, where a plateau develops in the T_c versus doping curve, $T_c(x)$. [17, 18] In addition, magnetization and penetration depth results have recently been reported to behave anomalously at $x = \frac{1}{8}$. [19] The above phenomena have been attributed by various authors to a stripe phase known to exist in these compounds. [20] The connection with stripes emerges from the fact that at $x = \frac{1}{8}$ the stripe spacing is commensurate with the underlying crystal structure. We note in passing, that anomalies are expected also for other x values at which commensurability conditions prevail, often referred to as magic numbers. [21]

Following the above considerations, we performed a systematic STS study of LSCO over a wide range of doping and temperature. To the best of our knowledge, this is the first report on STS measurements of the temperature evolution of the DOS in underdoped and overdoped LSCO, and for the $x = \frac{1}{8}$ doping level in particular. Our main findings are that the PG in LSCO pertains only to the underdoped regime, and is absent for doping levels higher than optimal. Additionally, for c -axis films with $x = 0.12$, a zero bias conductance peak (ZBCP) was observed on large smooth c -axis areas of the sample surface, replacing the expected V-shaped (c -axis tunneling) gap. This is a surprising result, since the ZBCP is known to be the dominant spectral feature on (110) surfaces due to the formation of Andreev bound states, while in c -axis tunneling spectra no such ZBCP is expected.

II. EXPERIMENT

90 nm thick LSCO films were epitaxially grown on (100) $SrTiO_3$ wafers by laser ablation deposition, with c -axis orientation normal to the substrate. About three films for each of the following doping levels were measured: $x = 0.08, 0.10, 0.12$ (underdoped); $x = 0.15$ (optimally doped) and $x = 0.18$ (overdoped). The LSCO films consisted of c -axis crystallites having well defined facets, 50 - 100 nm long, as shown in Fig. 1(a). As will be detailed below, most of the exposed side facets are (100) oriented, but some exposed side facets are of the (110) surface. The samples were transferred from the growth chamber in a dry atmosphere and introduced into our cryogenic STM after being exposed to ambient air for less than 5 min. About six tunneling spectra (dI/dV vs. V characteristics) were acquired at each position to assure data reproducibility. We also checked the dependence of the tunneling spectra on the voltage and current settings (i.e., the tip-sample distance, or the tunneling resistance values, in the range of 100 M Ω to 1 G Ω) and found no effect on the measured gap features, disproving the possibility that these gaps are even partially related to single electron charging effects. [22] The temperature dependent resistance [$R(T)$] measurements were performed using the standard 4-probe technique, where special care was taken to stabilize the temperature before each resistance measurement and to avoid sample heating.

III. RESULTS AND DISCUSSION

A. Evolution of the gap structure with doping and temperature

For all the doping levels studied, except for $x = 0.12$ (see below), the tunneling spectra measured on top of the LSCO crystallites exhibited V-shaped gap structures typical of c -axis tunneling, further confirming the assigned crystallographic orientation found by X-ray diffraction. A typical spectrum is presented in Fig. 1(b) along with a fit to the model for tunneling into a d -wave superconductor. [23] In many cases, the spectra acquired on the crystallite side facets portrayed a U-shaped gap structure [see Fig. 1(c)], signifying tunneling into *smooth* (100) facets, as discussed in Ref. 24. Finally, as depicted by Fig. 1(d), along some of the side facets, we have measured ZBCPs (usually inside a gap-like structure), suggesting that the corresponding facet exposes the (110) surface, or at least that tunneling

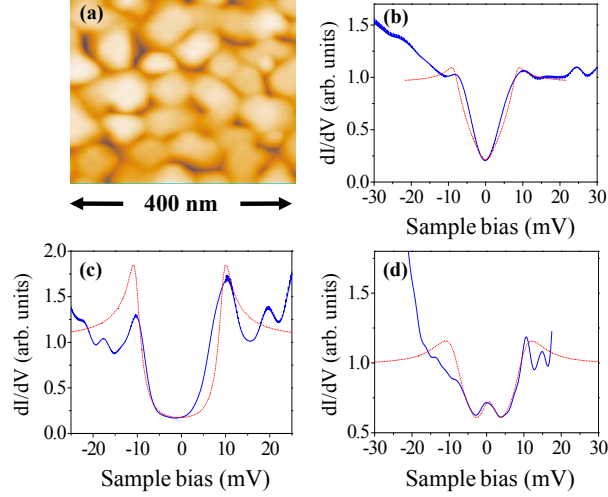


FIG. 1: (a) $400 \times 400 \text{ nm}^2$ topography image of $x = 0.08$ LSCO film. (b-d) Tunneling spectra at 4.2 K (blue curves) taken on a single crystallite. The spectrum in (b) was measured at the top of the crystallite and shows a typical c -axis V-shaped gap structure. The spectra in (c) and (d) were acquired on two different facets of the crystallite. The one in (c) portrays a U-shaped gap, typical for tunneling into a *smooth* (100) facet, and that in (d) exhibits a ZBCP, signifying that the tunneling took place out of the anti-nodal direction. The dotted red lines are fits to the theory of tunneling into a d -wave SC.

takes place in the a - b (CuO_2) plane in a direction different from $[100]$. Indeed, the dotted red line in Fig. 1(d) was calculated using the aforementioned model [23] assuming tunneling to the a - b plane at an angle of $\frac{\pi}{3}$ with respect to the $[100]$ axis. A similar correlation between the tunneling spectra and the surface nano-morphology was observed in our previous investigations of YBCO films. [25] The ZBCP, a unique spectral feature of d -wave SCs, [26] will be further discussed below. Interestingly, pronounced above-gap structures appear in the tunneling spectra that were acquired on the side facets of the c -axis crystallites [spectra (c) and (d)]. Such features occasionally appear, in a weaker manner, also in the c -axis (on crystallite) tunneling data. These above-gap features may be related to the phonon structure, which may be more efficiently detected when tunneling into the a - b plane. [27]

In fig 2 we present differential conductance spectra acquired at selected temperatures on three samples: a heavily underdoped $x = 0.08$ (a), an optimally doped $x = 0.15$ (b) and an overdoped $x = 0.18$ (c), samples. The gap value, Δ , was extracted from the data by taking half the width between the coherence peaks. At temperatures higher than 4.2 K,

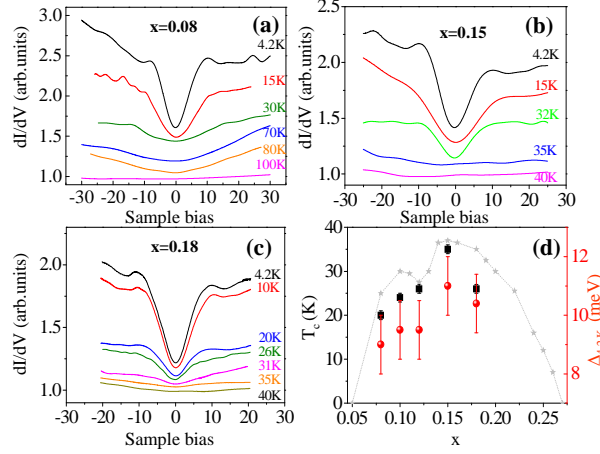


FIG. 2: (a-c) Tunneling dI/dV vs. V curves (shifted vertically for clarity) at various temperatures and for three different doping levels: (a) $x = 0.08$ (underdoped, $T_c \approx 20$ K); (b) $x = 0.15$ (optimally doped, $T_c \approx 35$ K); (c) $x = 0.18$ (overdoped, $T_c \approx 29$ K). (d) The 4.2 K gap (red circles, right axis) and T_c (black squares, left axis) as a function of doping. For comparison we plot $T_c(x)$ measured on LSCO single crystals from T. Matsuzaki, Phys. Chem. Sol. **62**, 29 (2001).

where the coherence peaks were smeared, the maximum change of the slope was taken as the position of the gap edge. This method, which yields some uncertainty in the determination of the gap values, was applied before for tunneling spectra obtained on LSCO, since in many cases the coherence peaks were undetectable. [28] Fig. 2(d) summarizes the $\Delta_{4.2K}$ values (red circles, right axis) and the measured T_c values (black rectangles, left axis) for all the doping levels measured. The error bars associated with the gap data represent the range of spatial fluctuations in the $\Delta_{4.2K}$ values, whereas those corresponding to T_c reflect the width of the transition. For reference we have added the $T_c(x)$ values measured on single crystals (asterisks and dotted line) from Ref. 17. The systematic lower T_c values measured on our thin films, as compared to those of the single crystals, is probably due to strain forces generated by the mismatch between the lattice constants of the $SrTiO_3$ substrate and the LSCO film. [18, 29] The evolution of Δ with doping appears to follow the SC dome structure. This appears to be a reasonable result, if the gap magnitude is related to the pair potential of the Cooper pairs that, in turn, is associated with T_c . It should be emphasized, however, that there are reports of STS data showing different behaviors. [4, 30] We note in passing that our observation for the doping dependence of $\Delta_{4.2K}$ is similar to that of the peak in the Raman spectra associated with nodal-quasiparticles excitations, reported

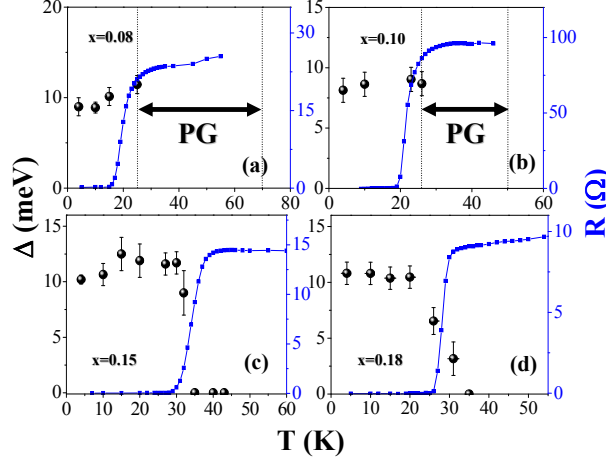


FIG. 3: Summary of the SC gap width evolution with temperature for underdoped samples, $x = 0.08$ (a) and $x = 0.10$ (b), optimally doped, $x = 0.15$ (c) and overdoped, $x = 0.18$ (d) samples. The gaps (black circles, left axes) are plotted along with the $R(T)$ data (blue squares and lines, right axes) for each doping level. The double sided arrow in (a) and (b) marks the temperature range where the PG was clearly detectable as a depression in the tunneling spectra. At the right hand side of the double sided arrow (T^*) the zero-bias conductance increases toward the normal conductance and consequently the gap structure vanishes. These data show that the PG exists only for underdoped samples.

in Ref 31. The origin of this correspondence is not yet clear to us. Moreover, we do not find evidence for the two energy scales discussed in the latter paper, maybe because c -axis tunneling spectroscopy probes *simultaneously* the anti-nodal and nodal excitations.

Fig 3 summarizes the evolution with temperature of the SC gap width (below T_c) for different doping levels. The gap values (black circles, left axes) were extracted from the differential conductance curves, as explained above. The error bars represent standard deviations of the spatial distribution of the gap magnitude and the error in determining the gap value when the coherence peaks are absent, as discussed above. For each doping level we present the corresponding $R(T)$ curve that was measured right after the STM measurements. As seen in Fig. 2(a), the SC gap of the underdoped $x = 0.08$ films does not close up at T_c , as a BCS gap would. Instead, the gap evolved smoothly into a PG, manifested by a depletion in the density of states around E_F . The PG that was noticeable up to $T^* \sim 70$ K, well above the onset temperature of superconductivity, $T_c^{onset} \sim 30$ K. The smearing of the gap edges at $T > T_c$ created large errors in the determination of the (pseudo)gap width,

therefore we do not plot the gap values. Nevertheless, the temperature range where the PG was clearly detectable is presented in Fig. 3(a) as a double sided arrow, starting at T_c and ending at the temperature, T^* , where the spectra turned gapless (or Ohmic). Qualitatively, a similar behavior was observed for the (still underdoped) $x = 0.10$ samples, with $T^* \sim 50$ K [Fig. 3(b)].

The results of the optimally doped and overdoped films are shown in Figs. 3(c) and 3(d). As in the case of the underdoped samples, the SC-gap width remains almost constant nearly up to T_c . However, in contrast with the underdoped films, the gap in the DOS closes up and vanishes near T_c , while no sign of the PG is observed. The behavior of the overdoped ($x = 0.18$) differs even more profoundly from that of the underdoped samples. As can be seen in Figs. 2(c) and 3(d), the width of the SC gap (as well as its depth) reduced significantly already at $\sim \frac{2}{3}T_c^{onset}$, and completely disappears at $T_c^{onset} \sim 31$ K. This behavior resembles the temperature evolution of a BCS-like gap. [32] Our data may thus portray a crossover from a non-BCS to a BCS-like SC gap behavior as the doping increases from below to above optimal doping, as suggested previously. [33, 34]

We conclude that our STS results corroborate earlier findings on LSCO (using other experimental methods) as well as on other cuprates, showing that the PG is an intrinsic property of the underdoped regime. However, both the doping dependence of the gap magnitude and the restriction of the PG to the underdoped regime exclusively, are in contrast to findings by Renner et al. for BSCCO. [4] These authors found clear evidence for a PG in overdoped BSCCO samples (while we do not) and reported that Δ monotonically decreased as the doping level was increased (whereas we found that Δ follows the SC dome, see Fig. 2). These discrepancies lead one to question the universality of the SC gap and PG attributes among the family of the HTSC cuprates. We note that the cuprates differ from one another in various ways, e.g., in the number of CuO_2 planes within the unit cell, the T_c values and the doping methods, thus universality should not necessarily prevail.

B. Anomalous behavior at $x = 0.12$

When examining c -axis LSCO films with $x = 0.12$ ($\approx \frac{1}{8}$) we encountered a surprising effect. The local tunneling spectra over large areas of the sample, including those measured *on top* of c -axis crystallites, exhibited ZBCPs instead of the expected c -axis V-shaped

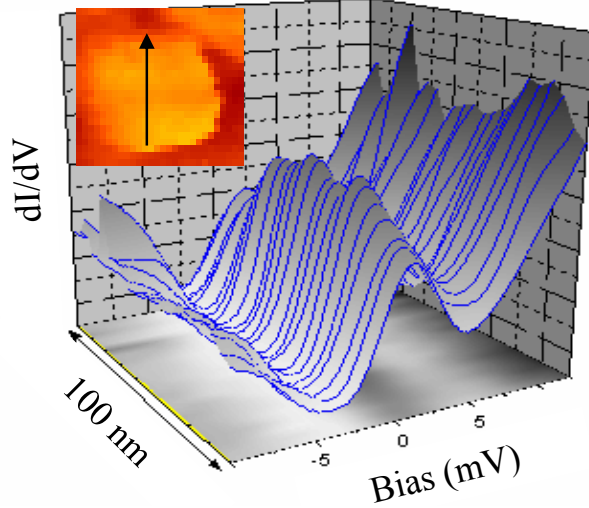


FIG. 4: Tunneling spectra measured at 4.2 K on a c -axis $x = 0.12$ LSCO film. The spectra were taken sequentially at equidistant steps (~ 4 nm) along the 100 nm long line running on top of a c -axis crystallite, as shown in the inset. Surprisingly, the spectra exhibit a ZBCP instead of a pure V-shaped gap structure.

tunneling gap. In Fig. 4 we present a typical line scan taken on top of a c -axis crystallite (shown in the inset) in one of our $x = 0.12$ films. All the spectra indeed exhibit clear ZBCP structures. This behavior was observed for all three $x = 0.12$ samples we measured, on different locations on each film separated by a few millimeters from one another and for various directions of the line-scan. Areas showing the expected (ZBCP-free) gap structure were also found, but they comprised less than 15% of the scanned sample area [the corresponding data were used in the analysis shown in Fig. 2(d)]. We would like to emphasize that the unexpected appearance of the ZBCP was exclusively found in the $x = 0.12$ doping level, whereas for other doping levels only V-shaped gaps were observed on top of the crystallites (see Fig. 1). In the latter ($x \neq 0.12$) films, the ZBCPs were detected only along some of the crystallite facets, as discussed above.

The ZBCP spectral feature is one of the hallmarks of d -wave superconductivity. [23, 26] It originates from the formation of zero-energy (at E_F) surface bound states, known as Andreev bound states (ABS). The ABS appear on the nodal surfaces of d -wave superconductors [(110) in LSCO and YBCO] due to constructive interference of multiple Andreev reflected quasiparticles that experience a sign change of the order parameter in consecutive reflections. [23, 26] The ZBCP is *not* expected to be observed in spatially

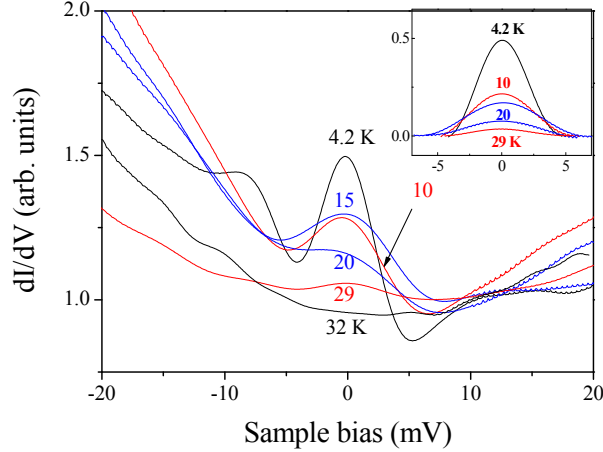


FIG. 5: Tunneling spectra curves at various temperatures measured on an $x = 0.12$ LSCO film. Inset: The ZBCPs after background subtraction.

resolved STS data acquired on top of c -axis crystallites, but can be detected on side facets of these crystallites, as demonstrated above and even more clearly on pure (110) facets. [25]

We believe that the anomalous abundance of ZBCPs reported here for the $x = 0.12$ films cannot be associated with faceting and local tunneling along the nodal [110] direction (in spite of the fact that they look very similar to the nodal, ABS-related, ZBCPs). As noted above, line scans continuously showing ZBCPs were measured along different directions (that did not necessarily run along any major crystallographic direction) on a single crystallite. In addition, no ZBCP were found on-top of crystallites in the films of other ($x \neq 0.12$) doping levels, indicating that the presence of (110) nano-facets is negligible in our films. These findings practically rule out the possibility that the ZBCPs are associated with (110) facets. Moreover, X-ray diffraction measurements on our samples revealed highly oriented c -axis films with sharp (00n) peaks and no other orientations.

Next we address the temperature evolution of the ZBCP in the $x = 0.12$ films. As demonstrated in Fig. 5, the magnitude of the ZBCP gradually decreases as the temperature is raised and vanishes at about 30 K, very close to (and slightly above) the SC transition temperature. In order to compare the 'anomalous' ZPCPs with the 'conventional' ones associated with the nodal ABS, we have performed temperature dependent STS measurements on $x = 0.12$ LSCO films grown intentionally on (110) STO wafers. X-ray diffraction measurements showed that in addition to the (110) LSCO orientation, a large amount of (103) orientation is also present in these films. This however posed no problem since, as

previously shown, ZBCPs due to ABS exist also for this orientation. [35, 36] Fig. 6 displays a comparison between the temperature evolution of the ZBCP magnitude measured on (001) and nominal (110) films. Each data point in this figure represents the integrated area under the corresponding ZBCP after subtraction of the background conductance as shown in the inset of Fig. 5. Assuming that the ZBCP observed on the c -axis film is also due to some type of zero-energy surface bound states, the data in Fig. 6 reflect the number of bound states at each temperature. [37] Both sets of data show that the ZBCP magnitude decreases monotonically as the temperature is increased. There is, however, a marked difference between the two samples, namely, the two types of ZBCPs. While the ZBCPs on the (001) surface were still detectable at around $T_c \approx 27\text{K}$, the 'conventional' ZBCPs vanished already at a much lower temperature, $\sim 18\text{ K}$, well below T_c .

Previous tunneling spectroscopy investigations of the nodal surfaces of LSCO and YBCO showed that the ABS usually lose all spectral weight at about $0.5 - 0.6T_c$. [13, 38] In particular for the (110) surface of an $x = 0.12$ LSCO single crystal, Dagan et al. have shown, using point contact spectroscopy, that the ZBCP disappeared at $\sim 15\text{ K}$, while T_c was $\sim 31\text{ K}$. The qualitative agreement of this finding with our results for the nominal (110) surface [Fig. 6(b)] on one hand, and the different behavior we found for the 'anomalous' (001)-surface ZBCPs [Fig. 6(a)] on the other hand, further support our claim that the $x = 0.12$ anomaly is not a faceting effect. Nevertheless, the fact that the 'anomalous' ZBCPs have a similar shape to that of the nodal ones and that they also quench with increasing temperature suggests that they also manifest surface bound states resulting from multiple Andreev reflections. The exact mechanism (or multiple Andreev reflection process) that underlines the formation of these bound states is probably different from that associated with the nodal ABS [26] and has not been predicted or discussed in the literature as of yet.

Bobkova et al. predicted theoretically that zero-energy bound states should exist at the interface between the a - b plane of a d -wave SC and a charge density wave (CDW) material, provided this junction has high enough transparency. [39] These bound states represent a combined effect of Andreev reflections from the superconducting side, unconventional Q-reflections from the CDW solid, and standard specular reflections. In a Q-reflection from the interface with the CDW solid, a sub CDW-gap quasiparticle changes its momentum by the wavevector Q of the CDW pattern. While this model is not directly

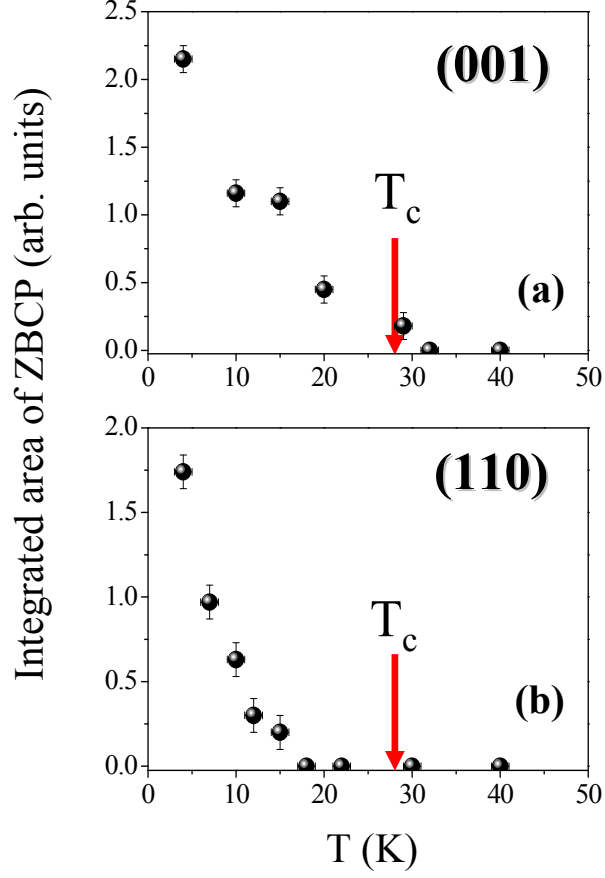


FIG. 6: The temperature dependence of the spectral weight the ZBCPs measured on the (001) (a) and (110) (b) films. The (001) ZBCP vanished at around T_c , whereas that measured on the (110) film vanishes at a lower temperature, as commonly found for ZBCPs associated with the 'conventional' nodal ABS.

related to our experimental configuration, it may indicate a possible direction at which a relevant model could be established, namely, the involvement of static stripes. Neutron scattering measurements have shown the existence of static stripes commensurate with the underlying crystal structure in LSCO for $x = \frac{1}{8}$. [20] These stripes exhibit charge modulation that can be related to a CDW order parameter, which coexists with a d -wave order parameter. A serious theoretical investigation is thus needed on the possible role of stripes in the appearance of the ZBCP anomaly that we observed in the $x = \frac{1}{8}$ LSCO films.

IV. SUMMARY

In conclusion, we have shown that the PG in epitaxial thin films of LSCO exists only in the underdoped regime where above T_c , the gap became more and more shallow and eventually vanished at a doping dependent temperature $T^* > T_c$. At 4.2 K the SC gap magnitude was found to qualitatively follow the SC dome structure versus doping, as expected for a gap magnitude proportional to the pairing potential. The disagreement of our results with those obtained on BSCCO suggests that the SC gap and PG properties may not be universal among the HTSC cuprates. We have also revealed a new anomaly associated with the special $x = \frac{1}{8}$ doping level of LSCO. The c -axis tunneling spectra exhibited a predominant ZBCP instead of the expected V-shaped gap, manifesting the creation of a new type of zero energy bound states. Ruling out the possibility that this is a facet effect, we conjecture that this anomalous spectral feature is associated with static stripes. Further theoretical modeling and experimental data using different methods are needed in order to resolve the puzzle associated with this intriguing effect.

V. ACKNOWLEDGMENTS

The authors are grateful to G. Deutscher, D. Orgad, and S. Baruch, for helpful and stimulating discussions. This research was supported by the Israel Science Foundation, Center of Excellence program (grant # 1565/04).

-
- [1] T. Timusk and B. Statt, Rep. Prog. Phys. **62**, 61 (1999).
 - [2] A. Ino, T. Mizokawa, K. Kobayashi, and A. Fujimori, T. Sasagawa, T. Kimura, K. Kishio, K. Tamasaku, H. Eisaki and S. Uchida Phys. Rev. Lett, **81**, 2124 (1998).
 - [3] T. Sato, T. Yokoya, Y. Naitoh, T. Takahashi, K. Yamada and Y. Endoh, Phys. Rev. Lett, **83**, 2254 (1999).
 - [4] C. Renner, B. Revaz, J.-Y. Genoud, K. Kadowaki and Ø. Fischer, Phys. Rev. Lett, **80**, 149 (1998).
 - [5] M. Kugler, Ø. Fischer, C. Renner, S. Ono and Y. Ando Phys. Rev. Lett, **86**, 4911 (2001).

- [6] I. Maggio-Aprile, C. Renner, A. Erb, E. Walker, B. Revaz, J.-Y Genoud, K. Kadowaki and Ø. Fischer, *J. Elec. Spec. Rel. Phen.*, **109**, 147 (2000).
- [7] K. M. Lang, V. Madhavan, J. E. Hoffman, E. W. Hudson, H. Eisaki, S. Uchida and J. C. Davis, *nature*, **415**, 24 (2002).
- [8] J. E. Hoffman, K. McElroy, D.-H. Lee, K. M Lang, H. Eisaki, S. Uchida and J. C. Davis, *science*, **297**, 1148 (2002).
- [9] M. Vershinin, S. Misra, S. Ono, Y. Abe, Y. Ando and A. Yazdani, *science*, **303**, 1995 (2004).
- [10] C. Howald, H. Eisaki, N. Kaneko, M. Greven and A. Kapitulnik, *Phys. Rev. B* **67**, 014533 (2003).
- [11] S. R. Curras, G. Ferro, M. T. Gonzalez, M. V. Ramallo, M. Ruibal, J. A. Veira, P. Wagner and F. Vidal, *Phys. Rev. B* **68**, 094501 (2003).
- [12] R.S. Gonnelli, A. Calzolari, D. Daghero, L. Natale, G.A. Ummarino, V.A. Stepanov and M. Ferretti, *Eur. Phys. J. B* **22**, 411 (2001).
- [13] Y. Dagan, A. Kohen, G. Deutscher and A. Revcolevschi, *Phys. Rev. B* **61**, 7012 (2000).
- [14] N. L. Wang, P. Zheng, T. Feng, G. D. Gu, C. C. Homes, J. M. Tranquada, B. D. Gaulin and T. Timusk, *Phys. Rev. B* **67**, 134526 (2003).
- [15] A. Damascelli, Z. Hussain and Z.-X. Shen, *Rev. Mod. Phys.* **75**, 473 (2003).
- [16] A. R. Moodenbaugh, Y. Xu, M. Suenaga, T. J. Folkerts and R. N. Shelton, *Phys. Rev. B* **38**, 4596 (1998).
- [17] T. Matsuzaki, M. Ido, N. Momono, R.M. Distaso, T. Nagata, A. Sakai and M. Oda, *J. Phys. Chem. Sol.* **62**, 29 (2001).
- [18] H. Sato, A. Tsukada and M. Naito, *Physica C* **408-410**, 848 (2004).
- [19] C. Panagopoulos, M. Majoros, T. Nishizaki and H. Iwasaki, *Phys. Rev. Lett.* **96**, 047002 (2006).
- [20] E. W. Carlson, V. J. Emery, S. A. Kivelson and D. Orgad, *condmat* **0206217**, (2007) Review chapter to appear in ‘The Physics of Conventional and Unconventional Superconductors’ ed. by K. H. Bennemann and J. B. Ketterson (Springer-Verlag) .
- [21] S. Komiya, H.-D. Chen, S.-C. Zhang and Y. Ando, *Phys. Rev. Lett.* **94**, 207004 (2005).
- [22] E. Bar-Sadeh and O. Millo, *Phys. Rev. B* **53**, 3482 (1996).
- [23] S. Kashiwaya, Y. Tanaka, M. Koyanagi and K. Kajimura, *Phys. Rev. B* **53**, 2667 (1996).
- [24] A. Sharoni, G. Leibovitch, A. Kohen, R. Beck, G. Deutscher, G. Koren and O. Millo, *Eur.*

- Phys. Lett. **62**, 883 (2003).
- [25] A. Sharoni, G. Koren and O. Millo, Eur. Phys. Lett. **54**, 675 (2001).
 - [26] C.-R. Hu, Phys. Rev. Lett. **72**, 1526 (1994).
 - [27] S. Pilgram, T.M. Rice and M. Sigrist, Phys. Rev. Lett. **97**, 117003 (2006).
 - [28] T. Kato, S. Okitsu and H. Sakata, Phys. Rev. B **72**, 144518 (2005).
 - [29] G. Logvenov, I. Bozovic and I. Sveklo in *Proceedings of the International Society for Optical Engineering, San Diego, 2005* edited by I. Bozovic and D. Pavuna (San Diego, 2005), p. 59320Z-1.
 - [30] N. -C. Yeh, C.-T Chen, R. P. Vasquez, C. U. Jung, S.-I Lee, K. Yoshida and S. Tajima, J. Low. Temp. Phys. **131**, 435 (2003).
 - [31] M. Le Tacon, A. Sacuto, A. Georges, G. Kotliar, Y. Gallais, D. Colson and A. Forget, Nature Phys. **2**, 537 (2006).
 - [32] M. Tinkham, *Introduction to superconductivity* (Dover publications inc., New York, 2004), p. 64.
 - [33] G. Deutscher, nature **397**, 410 (1999).
 - [34] Y. J. Uemura, Physica C **282-287**, 194 (1997).
 - [35] M. Covington, M. Aprili, E. Paraoanu, L. H. Greene, F. Xu, J. Zhu and C. A. Mirkin, Phys. Rev. Lett. **79**, 277 (1997).
 - [36] J. Lesueur, X. Gison, M. Aprili and T. Kontos, J. Low. Temp. Phys. **117**, 539 (1999).
 - [37] I. Asulin, A. Sharoni, O. Yulli, G. Koren and O. Millo, Phys. Rev. Lett. **93**, 157001 (2004).
 - [38] H. Aubin, L. H. Greene, S. Jian and D.G. Hinks, Phys. Rev. Lett. **89**, 177001 (2002).
 - [39] I. V. Bobkova and Yu. S. Barash, Phys. Rev. B **71**, 144510 (2005).